http://dx.doi.org/10.5012/bkcs.2012.33.2.511

Hyperpolarized ^{129}Xe NMR Study of TiO_2 Nanotubes

Sang Man Lee,[†] Soon Chang Lee,[‡] Vandana Mehrotra,[†] Hae Jin Kim,[‡] and Hee Cheon Lee[†,*]

[†]*Department of Chemistry, Pohang University of Science and Technology, Pohang 790-784, Korea.* [*]*E-mail: hcl@postech.ac.kr*
[‡]*Energy & Applied Nano Material Research Team, Korea Basic Science Institute, Daejon 305-333, Korea*
Received November 19, 2011, Accepted December 7, 2011

A continuous flow hyperpolarized (HP) ^{129}Xe NMR spectroscopy was employed for the first time to investigate TiO_2 nanotubes (Ti-NTs) synthesized from commercial nanoparticles with different reaction times. A single peak attributing to channels for Ti-NTs was observed for variable temperature HP ^{129}Xe NMR spectra. It was also noted that there is alteration in value for heat of adsorption, ΔH from 12.6 ± 1.3 to 16.4 ± 0.4 kJ/mol and variation in chemical shift of the xenon adsorbed in channels, δ_s from 120 ± 2 ~ 135 ± 9 ppm which were closely correlated to channel length and it was shown that P25-24 Ti-NTs with longest channel is most favorite Ti-NTs for Xe adsorption.

Key Words : NMR, Hyperpolarization, Xenon, TiO_2, Nanotubes

Introduction

Since the discovery of carbon[1] and non-carbon nanotubes,[2] a lot of research has been carried out producing nanotubes with unique and novel properties such as electronic and thermal conductivity, gas adsorption and selectivity. Due to these attractive characteristics, non-carbon nanotubes have been produced and developed into conducting nanotubes through various synthesized methods.[2,3] TiO_2 nanotubes (Ti-NTs) are especially expected to have useful geometrical properties inherited from its one dimensional structure, the photo-catalytic effects along with semiconductive nature from TiO_2.[4] Therefore, it is a source of interest in many applications like solar cell,[5] energy storage in batteries[6] and nano-bio engineering such as nano-sensors,[7] nano-reactor and nano-electronics.[8] Although various methods such as N_2 adsorption isotherms, X-ray diffraction (XRD), high resolution transmission electron microscopy (HR-TEM) and selected area electron diffraction (SAED) have been used to investigate characteristics of Ti-NTs, their theory of formation and chemical structure has hardly been explicitly explained up till now.

^{129}Xe NMR is a traditional technique for porous materials to identify their absorption sites, molecular access and adsorption. The large chemical shift range and inert properties of ^{129}Xe have made it a powerful and favorable tool to investigate them strongly based on the physical environment and chemical composition of the local sites in the molecules.[9] However, the sensitivity of xenon under thermal equilibrium conditions is too low to observe interactions between xenon and local environment at very low concentration due to the low nuclear spin density of the gas. Hyperpolarized (HP) xenon obtained by optical pumping enables to overcome this obstacle by increasing xenon sensitivity up to a factor of 10^4-10^5.[10] Furthermore, HP ^{129}Xe NMR combined with the continuous flow method can minimize the contribution of Xe-Xe interaction to ^{129}Xe chemical shifts, providing more accurate information on xenon-pore interaction. Lately, HP ^{129}Xe NMR on TiO_2 nanorod was demonstrated by Wang *et al.*,[11] who reported the porosity and interconnectivity of pores in crystalline meso-porous TiO_2. In this study, HP ^{129}Xe NMR spectroscopy has been used for the first time with continuous flow system to characterize the channels in Ti-NTs.

Experimental

The commercial TiO_2 powders (Degussa P25, Germany) were purchased for the synthesis of Ti-NTs. These nanoparticles are nano-crystalline composed of 80% anatase and 20% rutile phases with surface area of 49 m^2/g and primary particle size of 25-30 nm.[12] Ti-NTs were synthesized by a hydrothermal reaction according to the previous method.[13] In a typical synthetic method, 0.2 g of nanoparticles were mixed with 20 mL of 10 M aqueous solution of NaOH in a parafilm-sealed polypropylene bottle followed by hydrothermal treatment in a heating oven at 120 °C for different reaction times (12, 24, 36 and 48 h). Subsequently the powder was washed thoroughly with 0.1 M aqueous solution of HCl till pH 3, and then it was filtered and washed with distilled water and finally dried in a vacuum oven at 60 °C for one or two days. All synthesized Ti-NTs with different reaction time are shown in Table 1.

A home-built optical pumping system with a fiber coupled diode array laser (Coherent, USA) delivering 40 W power at 795 nm was used for the generation of HP xenon gas used in HP ^{129}Xe NMR. The sample was placed in a home-built 10 mm NMR tube designed for the homogeneous distribution of xenon gas. The gas mixture of 5% xenon, 10% nitrogen and the balanced helium[14] was introduced into the 10 mm NMR tube *via* 1/16 inch Teflon tubing under *ca*. 100 mL/min flow rate at 4 atm. to deliver HP xenon gas to the sample. Using this system, the optimized nuclear spin polarization of xenon is about 7%, which is approximately 10,000 times

Table 1. Average channel length, ΔH and δ_s for various Ti-NTs depending on different synthetic condition

P25-n Ti-NTs[a]	Average channel length (nm)[b]	ΔH (kJ/mol)	δ_s (ppm)
P25-12 Ti-NTs	85 ± 32	13.8 ± 1.1	133 ± 7
P25-24 Ti-NTs	142 ± 57	16.4 ± 0.4	120 ± 2
P25-36 Ti-NTs	93 ± 44	14.5 ± 1.6	126 ± 9
P25-48 Ti-NTs	78 ± 20	12.6 ± 1.3	135 ± 9

[a]P25-n Ti-NTs indicates the type of precursor P25 with the reaction time of 'n' hrs for synthesis. [b]It was calculated by measuring the number of Ti-NTs with a specific length in TEM images.[16] (see supporting information)

larger than that of thermal xenon. All spectra in this paper were recorded on a super-wide bore AMX-300 spectrometer (Bruker, Germany) operating at 83.02 MHz for ^{129}Xe. The spectra were recorded with a 90° pulse of 10 μsec and relaxation delay of 1 sec. ^{129}Xe chemical shift was indicated with reference to gaseous xenon at 0 ppm. Temperature control was achieved by B-VT 1000 temperature control unit (Bruker, Germany).

Results and Discussion

The synthesized Ti-NTs were first examined by Field Emission Transmission Electron Microscopy (JEOL, Japan) shown in Figure 1. The TEM image of P25-24 Ti-NTs in Figure 1(a) with 10 nm resolution clearly displays synthesized materials like crystalline tubes in multiple layers with spacing about 0.8 nm enclosing hollow channels of around 6 nm diameter. Figure 1(b) with 50 nm resolution also shows that the meso-structure of as-synthesized Ti-NTs with multilayers could be described as hollow and chaotic multiwall nanotube aggregates with channels of various length and width along with in homogeneously distributed large intercrystalline pore. This morphological pattern suggests that apart from interlayer there are two principal adsorptive sites in Ti-NTs, first is channel along their length; and secondly an intercrystalline pore generated by aggregation of channel surfaces. The wide interlayer of Ti-NT's also couldn't absorb Xe gas as they are intercalated with water.[15] In addition; there is some change in channel length related with hydrothermal reaction time. For a comparison, Figure 1(b)-(d) show the TEM images with 50nm resolution for various Ti-NTs which were synthesized by hydrothermal reaction for 24, 36, and 48 hours, respectively. The channel length for all the samples was calculated by measuring the number of Ti-NTs with a specific length of TEM images.[16] The decreasing channel length of Ti-NTs was displayed very well in these samples with increasing reaction time.[17] Table 1 also shows P25-12 Ti-NTs with reaction time of 12 hours had much shorter channels contrary to P25-24 Ti-NTs, Thus 24 hours was considered to be an optimum reaction time for synthesis of longest channels (see supporting information) and data for 12 hrs were not considered further. It is sure that the effect of sonication during sample preparation for TEM[18] was minimized by sonicating various Ti-NTs simultaneously.

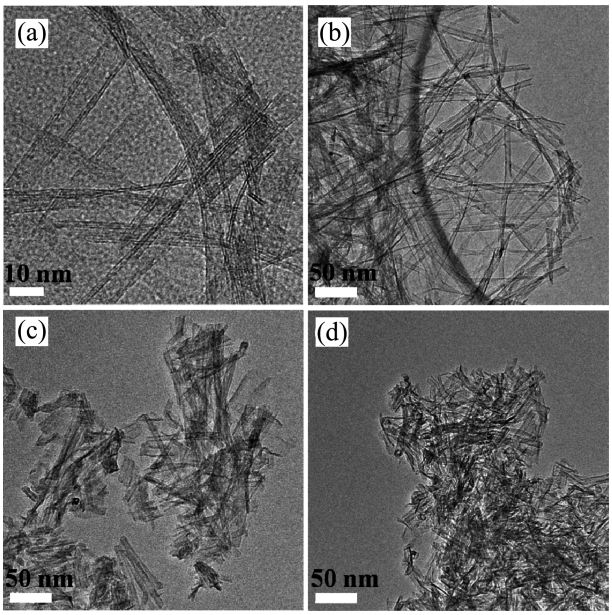

Figure 1. TEM images of (a) P25-24 Ti-NTs with 10 nm resolution, and (b) P25-24 Ti-NTs (c) P25-36 Ti-NTs and (d) P25-48 Ti-NTs with 50 nm resolution.

In order to investigate the quantitative relationship between HP ^{129}Xe NMR and Ti-NTs such as their channel length, we carried out variable temperature (VT) HP ^{129}Xe NMR experiment for a series of Ti-NTs using P25 nanoparticles as precursor. In Figure 2 for P25-24 Ti-NTs, only one xenon peak was detected with a small shoulder on the higher side of chemical shift above 310 K which can be assigned to intercrystalline pore.[19] In general, the observed ^{129}Xe chemical shift in high temperature region mainly depends on the mean pore diameter due to fast exchange between the adsorbed and free xenon gases which could be described as:[9]

$$\delta_{obs} = \langle \delta \rangle = (\delta_s \tau_s + \delta_f \tau_f)/(\tau_s + \tau_f) \quad (1)$$

where δ_s and δ_f are the chemical shifts of xenon adsorbed on

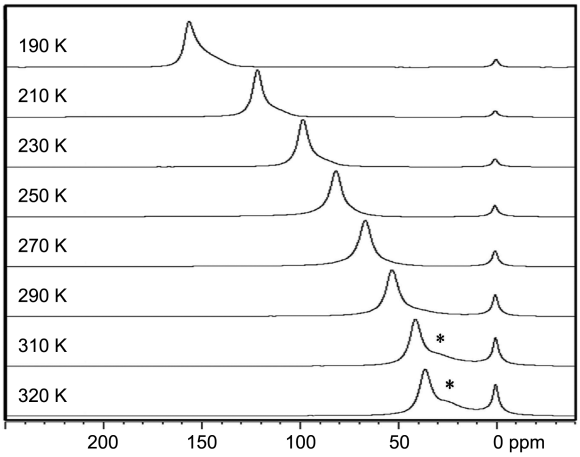

Figure 2. VT HP ^{129}Xe NMR spectra of P25-24 Ti-NTs. *indicates a shoulder peak originated from intercrystalline pores.

the surface and free gas, τ_s and τ_f are the mean residence time of xenon on the surface and free gas, respectively. When pore size is larger, the ^{129}Xe chemical shift on pore surface is diminished according to decreasing resident time of xenon and finally becomes too large to be distinguishable from xenon gas at 0 ppm. The ^{129}Xe chemical shift for P25-36 Ti-NTs and P25-48 Ti-NTs at 290 K is about 61 and 69 ppm, respectively and its linewidth around 680 Hz (see supporting information), while chemical shift and linewidth of P25-24 Ti-NTs are 53 ppm and 530 Hz, respectively, as shown in Figure 2. The ^{129}Xe chemical shift of Ti-NTs is strongly attributed to the change in its physical environments such as channels diameter or length if there is no change in their chemical compositions. The narrow xenon peak represents xenon adsorption in uniformly distributed system like channels rather than the intercrystalline pore. Thus, P25-24 Ti-NTs was observed to have largest surface and length of channels among various Ti-NTs. So, it could be concluded that the xenon peak would have originated from channels of Ti-NTs and ^{129}Xe chemical shift of Ti-NTs with longer channels is smaller than short channels. Xenon chemical shift for P25-24 Ti-NTs with the longest channels among various Ti-NTs is smallest at constant temperature in Figure 3 and this result is in good agreement with that of multi-wall CNT, in which long and short channels were observed at 43 ± 2 and 50 ± 2 ppm at 297 K, respectively.[20]

In order to classify the characteristics of various Ti-NTs specifically, we can calculate their heat of adsorption, ΔH and δ_s using the results of VT HP ^{129}Xe NMR in Figure 3. Based on Henry's Law, the correlation between ^{129}Xe chemical shift and temperature could be fit using fast exchange model with weak adsorption. Depending on mean pore diameter, D the observed chemical shift, δ_{obs} can be expressed as:

$$\delta_{obs}(T) = \delta_s\left(1 + D\left(\eta\kappa_0 R\sqrt{T}\exp\left(\frac{-\Delta H}{RT}\right)\right)^{-1}\right)^{-1} \qquad (2)$$

Where R, η and κ_0 are gas constant, pore geometry factor and pre-exponential factor, respectively. Table 1 shows that ΔH values of various Ti-NTs range from 12.6 to 16.4 kJ/mol, which is larger than 9.8 to 14.2 kJ/mol for previously reported TiO_2 porous nanorod.[11] It shows that formation of channels makes ΔH larger for other morphologies in Ti-NTs and ΔH for various Ti-NTs has a tendency to increase with increase in channel length. Therefore, it could be described that xenon adsorption of Ti-NTs with long channels is more favorable than amorphous TiO_2 materials without channels, besides P25-24 Ti-NTs with longest channels is most favorable adsorptive Ti-NT than any others. It can be concluded that the length of channels in Ti-NTs is most effective factor for xenon adsorption which is directly proportional to ΔH for all Ti-NTs.

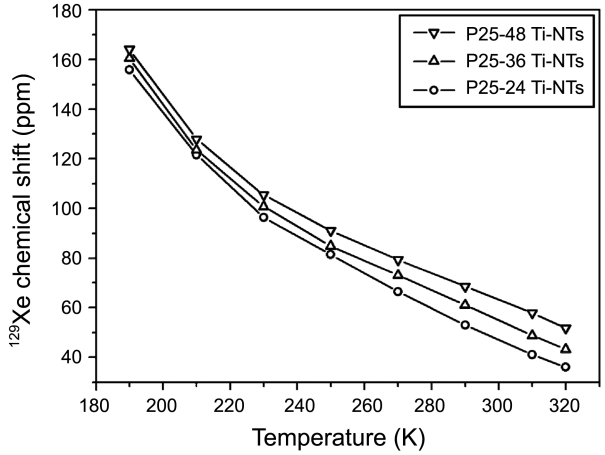

Figure 3. Plot of HP ^{129}Xe chemical shift as a function of temperature for various Ti-NTs.

On the other hand, the δ_s values of various Ti-NTs range from 120 to 135 ppm which is slightly larger than the range from 112 to 122 ppm for porous TiO_2 nanorod and 109 ppm for pure anatase nanoparticles.[11] Whereas formation of channels makes δ_s larger for other morphologies in Ti-NTs, δ_s for various Ti-NTs have a tendency to decrease with increase in channel length and δ_s for P25-24 Ti-NTs was calculated as the smallest value of 120 ± 2 ppm. In typical, δ_s can be attributed to both chemical environments as well as physical structure; the former was affected by the dissimilarity of chemical composition, the electronic state of Ti and the degree of hydration, while the latter depends on the surface roughness or the pore curvature. In the present case, since the chemical composition of synthesized Ti-NTs is identical to each other, variations of physical structure such as roughness or curvature could be dominant factors determining δ_s. Roughness is dependent on the surface heterogeneity which could result from shrinkage in channel length, while channel diameter makes its curvature change to a certain degree. As the change in diameter is too small to be observed, we can neglect its influence on the variation of δ_s. On the other hand, channel length directly affects the surface ratio of homogeneous inner channel to heterogeneous channel entrance and the roughness of Ti-NTs is closely dependent on this surface ratio. When channel length is larger, its surface ratio increases to diminish its degree of roughness. Therefore, overall δ_s for nanotubes with longer channel becomes smaller contrary to the heat of adsorption, ΔH which is directly proportional to length of channels.

Channel length conversely influences both two parameters, ΔH and δ_s effectively. P25-24 Ti-NTs, have largest heat of adsorption, ΔH and smallest chemical shift of xenon adsorbed in channel, δ_s. According to these results, there is a possibility for direct probe of various channel characteristics in nanotubes and obtaining indirect information about adsorption, catalysis or chemical reaction and microfluidic processes within channels using HP ^{129}Xe NMR.

Conclusion

Hyperpolarized (HP) ^{129}Xe NMR combined with a continuous flow method has been used to investigate TiO_2 nanotubes (Ti-NTs) synthesized from commercial nanoparticles with different reaction times. It was observed that only single xenon peak originated from well-defined adsorptive

site, channel of Ti-NTs which depends on their structural variation of channel length related with its hydrothermal reaction time. We also obtained largest ΔH and smallest δ_s values for the P25-24 Ti-NTs with longest channel length among all Ti-NTs using VT HP ^{129}Xe NMR spectra which makes P25-24 Ti-NTs most favorite for xenon adsorption.

Acknowledgments. This research was supported by Basic Science Research Program through the National Research Foundation of Korea (NRF) funded by the Ministry of Education, Science and Technology (2011-0004837).

Supplementary Materials. Supplementary figures are available at the bkcs website.

References

1. Iijima, S. *Nature* **1991**, *354*, 56.
2. Kasuga, T.; Hiramatsu, M.; Hoson, A.; Sekino, T.; Niihara, K. *Langmuir* **1998**, *14*, 3160.
3. Shamsi, M. H.; Geckeler, K. E. *Nanotechnology* **2008**, *19*, 5.
4. Ou, H. H.; Lo, S. L. *Separation and Purification Technology* **2007**, *58*, 179.
5. Kuang, D.; Brillet, J.; Chen, P.; Takata, M.; Uchida, S.; Miura, H.; Sumioka, K.; Zakeeruddin, S. M.; Gratzel, M. *ACS Nano* **2008**, *2*, 1113.
6. Xu, J.; Jia, C.; Cao, B.; Zhang, W. F. *Electrochimica Acta* **2007**, *52*, 8044.
7. Seo, M. H.; Yuasa, M.; Kida, T.; Huh, J. S.; Yamazoe, N.; Shimanoe, K. *Sensors and Actuators B: Chemical* **2011**, *154*, 251.
8. Jun, Y.; Zarrin, H.; Fowler, M.; Chen, Z. *International Journal of Hydrogen Energy* **2011**, *36*, 6073.
9. Springuel-Huet, M.; Bonardet, J. L.; Fraissard, J. *Applied Magnetic Resonance* **1995**, *8*, 427.
10. Long, H. W.; Gaede, H. C.; Shore, J.; Reven, L.; Bowers, C. R.; Kritzenberger, J.; Pietrass, T.; Pines, A.; Tang, P.; Reimer, J. A. *Journal of the American Chemical Society* **1993**, *115*, 8491.
11. Wang, L. Q.; Wang, D.; Liu, J.; Exarhos, G. J.; Pawsey, S.; Moudrakovski, I. *The Journal of Physical Chemistry C* **2009**, *113*, 6577.
12. Ohno, T.; Sarukawa, K.; Tokieda, K.; Matsumura, M. *Journal of Catalysis* **2001**, *203*, 82.
13. Yuan, Z. Y.; Su, B. L. *Colloids and Surfaces A: Physicochemical and Engineering Aspects* **2004**, *241*, 173.
14. Fukutomi, J.; Suzuki, E.; Shimizu, T.; Kimura, A.; Fujiwara, H. *Journal of Magnetic Resonance* **2003**, *160*, 26.
15. Suzuki, Y.; Yoshikawa, S. *Journal of Materials Research* **2004**, *19*, 982.
16. Bavykin, D. V.; Walsh, F. C. *J. Phys. Chem. C* **2007**, *111*, 14644.
17. Wang, D.; Zhou, F.; Liu, Y.; Liu, W. *Materials Letters* **2008**, *62*, 1819.
18. Bavykin, D. V.; Walsh, F. C. *J. Phys. Chem. C* **2007**, *111*, 14644.
19. Andrei, N.; Haddad, E.; Flavien, G.; Antoine, G. *Phys. Chem. Chem. Phys.* **2003**, *5*, 4473.
20. Romanenko, K. V.; Fonseca, A.; Dumonteil, S.; Nagy, J. B.; d'Espinose de Lacaillerie, J. B.; Lapina, O. B.; Fraissard, J. *Solid State Nuclear Magnetic Resonance* **2005**, *28*, 135.